Review Article
A review of phosphate oxygen isotope values in global bedrocks: Characterising a critical endmember to the soil phosphorus system

Andrew C. Smith[1]*, Verena Pfahler[2,3], Federica Tamburini[4], Martin S. A. Blackwell[3], and **Steven J. Granger[3]**

[1] National Environmental Isotope Facility, British Geological Survey, Keyworth, Nottingham, NG12 5GG, UK
[2] Smithsonian Tropical Research Institute, Apartado 0843–03092, Balboa, Ancon, Panama
[3] Rothamsted Research, North Wyke, Okehampton, Devon EX20 2SB, UK
[4] Institute of Agricultural Sciences, ETH Zurich, 8315 Lindau, Switzerland

Abstract

Understanding the phosphate oxygen isotope ($\delta^{18}O\text{-}PO_4$) composition of bedrock phosphate sources is becoming ever more important, especially in areas of soil research which use this isotope signature as a proxy for biological cycling of phosphorus (P). For many of these studies, obtaining a sample of the source bedrock or applied mineral fertiliser for isotope analysis is impossible; meaning there is now a demand for a comprehensive characterisation of global bedrock $\delta^{18}O\text{-}PO_4$ to support this work. Here we compile $\delta^{18}O\text{-}PO_4$ data from a wide range of global bedrocks, including 56 new values produced as part of this study and a comprehensive overview of those within the previously existing literature. We present $\delta^{18}O\text{-}PO_4$ data from the range of major phosphatic lithologies alongside as much metadata for the samples as could be gathered. Much of the data comes from bedrocks of marine sedimentary origin (< 1 Ma = > +22‰, > 540 Ma = ≈ +12‰), but we also present data from bedrocks associated with guano (range: +19.5 to +15‰) and igneous deposits (range: +12 to –0.8‰), both of which have distinct $\delta^{18}O\text{-}PO_4$ signatures due to their formation mechanisms. We show that where repeat measurements of the same formation have been undertaken, regardless of method or exact sample location, there is an average within formation error of ± 1.25‰. This is important, as is constitutes a reasonable level of uncertainty for phosphorus cycling studies which need to estimate bedrock $\delta^{18}O\text{-}PO_4$ composition based on the literature. In combination, this data set presents 284 $\delta^{18}O\text{-}PO_4$ values from 56 countries; a comprehensive starting point for researchers interested in understanding bedrock end member $\delta^{18}O\text{-}PO_4$.

Key words: bedrock / oxygen isotope / phosphate cycle / phosphorus / soils

Accepted December 08, 2020

Supporting Information available online

1 Introduction

Bedrock phosphate (PO_4) is the major source of mineral phosphorus (P) within most soil systems, either as the natural weathered parent material underlying the soil or in the form of an applied mineral fertiliser (*Ruttenberg*, 2003). The nature and amount of P in the bedrock, as well as the bedrock material itself, varies (*Van Kauwenbergh*, 2010), influencing soil P transformations during pedogenesis on a range of scales (*Walker* and *Syers*, 1976). It is therefore critically important to understand this endmember to the soil P system, not least for studies using the oxygen isotope signature of PO_4 ($\delta^{18}O\text{-}PO_4$) to ascertain the extent and mechanisms of P uptake and cycling within the soil–plant system (*Bauke*, 2021).

Bedrock phosphate (PO_4) deposits can be loosely grouped into three major categories based upon their formation mechanism; these are (1) marine sedimentary, (2) guano and (3) igneous. A fourth category, including bedrocks derived from the weathered remnants of the former categories, could also be classified (*Chernoff* and *Orris*, 2002a, 2002b; *Szilas*, 2002). (1) Marine sedimentary PO_4 is derived from the upwelling of P rich organic ocean sediments to the continental shelf and the release of P during the bacterial breakdown of these compounds (*Goldhammer* et al., 2011). The subsequent precipitation and reworking of P minerals, such as francolite (carbonate fluorapatite), forms highly enriched phosphorite beds, containing pellets and nodules of francolite (*Hiatt* and *Budd*, 2001; *Shemesh* et al., 1988). (2) Phosphorus rich guano deposits are comparatively small accumulations of excreta associated with large colonies of birds or bats. The breakdown of fresh guano by microorganisms produces a number of highly soluble P precipitates (*Szilas*, 2002). These deposits are vulnerable to secondary weathering either leaving surface deposits or leaching down into underlying bedrock and precipitating P rich carbonate apatites (*Ayliffe* et al., 1992; *Szilas*, 2002). (3) Igneous P rich deposits are normally found as sheets of intrusive alkaline crystalline rock associated with

* Correspondence: A. C. Smith; e-mail: andrews@bgs.ac.uk

carbonatites. These form during the crystallisation of high temperature calcic alkaline silicate melts (*Pufahl* and *Groat*, 2017; *Szilas*, 2002). Each of these different formation mechanisms leaves an oxygen isotope fingerprint on the PO_4 molecule, related to inorganic and organic processes involved during the formation of the P mineral phase.

The use of phosphate oxygen isotope (δ^{18}O-PO_4) signatures in environmental research is rapidly developing as a robust solution for environmental tracing of the P cycle (*Bauke*, 2021). Much recent work has focused on P uptake within soils and subsequent nutrient transfer to the biosphere, where P is one of the fundamental elements for life (*Davies* et al., 2014; *Tamburini* et al., 2014; *George* et al., 2017; *Pistocchi* et al., 2018), but also a major environmental pollutant especially when it enters waterways, acting to reduce natural P limitation and enhance eutrophication effects (*McLaughlin* et al., 2006). To fully understand P cycling and pollution dynamics it is important to have a reliable, natural, non-radiogenic tracer for the modern P cycle. Phosphorus only has one stable isotope, ^{31}P, rendering traditional stable isotope tracing impossible and leaving our understanding of environmental P cycling far behind that of carbon and nitrogen (*McLaughlin* et al., 2006). In recent years, a number of researchers have exploited the fact that most P in the environment is bound to oxygen (O). Looking at the δ^{18}O of different P compounds and/or pools can help elucidate the primary origin, and secondary physical and biological processes acting upon this molecule (*Blake* et al., 2005; *Jaisi* et al., 2010; *Tamburini* et al., 2012). In this way the δ^{18}O signature of different P pools has been used to try and assess the extent, rate and controls over P cycling between these pools and uptake/release from biota (*Helfenstein* et al., 2018), as well as to try and trace PO_4 sources and potential pollutants, including agricultural fertilisers and wastewater discharges (*Gooddy* et al., 2016; *Granger* et al., 2017, 2018; *McLaughlin* et al., 2006).

The δ^{18}O-PO_4 method relies upon the fact that P is mainly associated to O in the environment and that the P–O bond is normally very stable in the absence of biological activity (*O'Neil* et al., 2003). The δ^{18}O-PO_4 can be altered due to a sorting of heavier or lighter isotopologues. Sorting can occur during abiotic processes, however, the effects of these abiotic processes on the δ^{18}O-PO_4 are still under discussion and appear to cause minimal alteration of the δ^{18}O-PO_4 signature (*Jaisi* and *Blake*, 2010; *Jaisi*, 2013; *Li* and *Jaisi*, 2015). Biological uptake of P can also result in an isotopic effect due to a preference of microorganisms for the lighter isotopologue, so far, mainly negative fractionation factors have been reported. Phosphorus uptake by the bacteria *Escherichia coli*, for example, has a fractionation of about –3‰ (*Blake* et al., 2005). Whilst isotope effects associated with P uptake do lead to small changes in the δ^{18}O-PO_4, more pronounced shifts in δ^{18}O-PO_4 are observed due to enzyme cleavage of the P–O bond (*Blake* et al., 2005). The enzymes, which cleave the P–O bond, can be divided into two groups: phosphomono- and diesterases which lead to an exchange of 1–2 O atoms with water from the surrounding environment, and the intracellular enzyme inorganic pyrophosphatase, which leads to the complete exchange of all four O atoms in phosphate (*Blake* et al., 2005). Phosphomono- and -diesterases catalyse the hydrolysis of organic P into PO_4 and the δ^{18}O-PO_4 of the released PO_4 is typically depleted in ^{18}O. These enzymes include RNase, 5′-nucleotidase, DNase, alkaline and acid phosphatase and phytases, with fractionation varying between –30 and +20‰ (*Liang* and *Blake*, 2009, 2006; *Von Sperber* et al., 2014). Intracellular enzymatic hydrolysis by inorganic pyrophosphatase (*Cohn*, 1957) leads to equilibrium fractionation defined by Eq. (1) (*Pistocchi* et al., 2017), rearranged from *Chang* and *Blake* (2015):

$$E\delta^{18}O - PO_4 = -0.18T + 26.3 + \delta^{18}O_{H_2O}, \quad (1)$$

where $E\delta^{18}O\text{-}PO_4$ is the δ^{18}O of phosphate at equilibrium with O in water catalysed by inorganic pyrophosphatase, T is temperature in °C, and $\delta^{18}O_{H_2O}$ is the δ^{18}O of ambient water.

The exchange of O during the biological breakdown of the P–O bond, and subsequent changes to the δ^{18}O-PO_4 signature is a potent method for tracing the dominant mechanism of P cycling within the environment (*McLaughlin* et al., 2006). Where the enzyme inorganic pyrophosphatase is the primary enzyme responsible for this P–O breakdown, often considered an indication for microbial P cycling, we can define the expected Eδ^{18}O-PO_4 endmember, provided all relevant parameters remain constant [Eq. (1)]. But to be able to draw any concrete conclusions regarding P cycling we must also know the δ^{18}O-PO_4 value of the other endmembers of the system including importantly the δ^{18}O-PO_4 of inorganic and organic P sources (*George* et al., 2017; *Granger* et al., 2018, *Bauke*; 2021). The inorganic P may in natural systems comprise simply local bedrock P, but in agricultural settings this may include anthropogenically applied, exogenous, sources in the form of fertilisers. These inorganic fertilisers are sourced globally, from high P containing geological deposits. International scale fertiliser operations often target larger marine sedimentary and igneous deposits, while high P guano deposits are more commonly utilised locally, due to economies of scale (*Ayliffe* et al., 1992; *Mizota* et al., 1992; *Szilas*, 2002; *McLaughlin* et al., 2006). It is important that studies undertaking source apportionment obtain samples of those endmembers, however, this is often not possible. In these cases, only knowledge of the geology of the underlying bedrock or applied inorganic (and organic) P may be available. For this reason, a wide-reaching understanding of the δ^{18}O-PO_4 signature of a range of phosphatic lithologies of different ages, locations and formation histories would prove extremely useful when trying to establish a representative endmember value for uptake into the P cycle.

Here we present the most comprehensive archive of δ^{18}O-PO_4 data to date, collected both from existing studies and our own rock archive. We present as much formation, age, mineralogy and location information as could be obtained for the three major phosphatic rock types (Tabs. S1–3). We use these data to highlight trends within the data set, which will help with correct identification of endmember δ^{18}O-PO_4 values over a wide range of lithologies and locations.

2 Materials

This archive of δ^{18}O-PO_4 data from a range of global phosphatic lithologies is derived from data collated from numerous papers as well as 56 new samples analysed as part of this project. These additional samples were kindly provided from the collections of Don Appleton at the British Geological Survey (BGS), John McArthur (University College London), and the Rothamsted Research (Harpenden, UK) sample archive. Metadata for old samples and often those within the literature was at times sparse. Where possible, we used the available location information from the original papers and supplemented this using the comprehensive global phosphate data set of (*Chernoff* and *Orris*, 2002a, 2002b). This archive allows us to provide approximate location, age and mineralogy for many of the samples (Tabs. S1–3). These additional data should prove invaluable for researchers interested in understanding geographic distribution of the δ^{18}O-PO_4 values. It should be noted that the grid references provided for sample locations are often based on our best knowledge, not a recorded sampling location, and these location data may relate to a local town or region where the exact sampling location is unknown. For some of the oldest references very minimal metadata were supplied; in these cases we have presented only the approximate location (country), age and δ^{18}O-PO_4 values as presented in the original articles.

3 Methods

Over the last decades the preparation and analysis of samples for δ^{18}O-PO_4 has changed due to improved preparation methods and a switch from conversion to $BiPO_4$ and subsequent fluorination to the production of silver phosphate (Ag_3PO_4) and high temperature elemental analysis (*Vennemann* et al., 2002). These changes have been designed to both reduce the level of organic P available for hydrolysis (*Tamburini* et al., 2010) and enable the tracing of any hydrolysis through an isotope labelling technique. These changes have resulted in the robust extraction protocol used below, eliminating organic P, though a series of precipitation and dissolution stages and reducing NO_3-O isotope exchange by using hydrochloric rather than nitric acid extractions. There have also been changes in the reported value for NBS120c, which has been used to standardise much of the δ^{18}O-PO_4 data, especially in the marine palaeoclimate community (*Pucéat* et al., 2010). It is possible that this change in analytical methodology has led to a change in the recorded δ^{18}O-PO_4 ($\approx$ +2.2‰), and this should be considered when comparing data across methods (*Pucéat* et al., 2010). However, rather than attempting to apply a correction across our data set, we have reported the raw published data and the reference from which this data was obtained (Tabs. S1–3). For comprehensive analytical methodologies we direct the reader to the original articles and to *Vennemann* et al. (2002) for a review of the methods, and *Pucéat* et al. (2010) for discussion of potential isotope offsets between methods.

Below, we briefly describe the analytical procedure followed for the purification and analysis of samples which were part of this study. Samples were purified in two separate labs, Rothamsted Research, UK, and at the National Environmental Isotope Facility (NEIF), British Geological Survey (BGS), following the same procedure which broadly follows *Tamburini* et al. (2010). All isotope analysis was undertaken at the NEIF facility BGS, UK.

3.1 Purification and production of Ag_3PO_4

Bedrock samples were hand ground and subsampled. Approximately 0.5 g of material were added to 50 mL of 1 M HCl and shaken at room temperature for 16 h before filtering through a Whatman filter (grade GF/F) to remove any undissolved residue. The supernatant was retained for concentration and isotope analysis. From here we followed a modified *Tamburini* et al. (2010) method, but omitted the DAX-8 resin step as organic contamination was minimal in rock samples (*Granger* et al., 2018). Briefly, dissolved PO_4 was first precipitated as ammonium phospho-molybdate (APM), ensuring a pH of 1 with the addition of 1 mL of concentrated sulphuric acid. The APM was filtered and then dissolved in NH_4-citrate solution before PO_4 was precipitated as magnesium ammonium phosphate (MAP). The MAP precipitate was filtered and dissolved in 0.5 M HNO_3 and shaken with cation resin (AG 50 8X). The final precipitation stage was achieved by adding 7 mL of Ag-ammine solution to precipitate Ag_3PO_4. Precipitation was left to occur slowly at 40°C for at least 16 h, the precipitate was filtered before being oven-dried at 50°C.

3.2 Mass spectrometry

The analysis of Ag_3PO_4 was undertaken by weighing approximately 300 μg of Ag_3PO_4 into a silver capsule, in triplicate. The sample was then converted to carbon monoxide (CO) using a thermal conversion elemental analyser (TC-EA, ThermoFinnigan, Germany) at 1,400°C in the presence of glassy carbon. The product CO mixed with a helium carrier gas and was analysed on a Delta + XL mass spectrometer (ThermoFinnigan, Germany). All analysis was undertaken at the BGS. The δ^{18}O-PO_4 values were calculated by comparison to an internal Ag_3PO_4 standard, ALFA-1 (ALFA-1 = δ^{18}O VSMOW value of +14.2‰). In the absence of an international Ag_3PO_4 reference material, the value for ALFA-1 is derived by comparison to the Ag_3PO_4 standard 'B2207' (Elemental Microanalysis Ltd., England), which has been measured in an inter-laboratory comparison study to have a δ^{18}O value of +21.7‰ *versus* VSMOW. Triplicate repeats had a typical precision $\sigma \leq 0.4$‰; furthermore, sample purity was assessed by determining the CO yield compared with the yield of Ag_3PO_4 standards, and rejecting samples where this differed by 10% (*Tamburini* et al., 2010).

4 Results and discussion

4.1 Global distribution of samples

Within the presented data set we have samples from many of the major global PO_4 reserves including several sites which were/are responsible for the supply of bedrock PO_4 for commercial purposes. We also compile the currently available δ^{18}O-PO_4 dataset for sedimentary, igneous and guano derived bedrocks produced for purely scientific interest, creating

a highly diverse, data set (Tabs. S1–3). Figure 1 displays the sample locations and global distribution of the bedrocks in this study, for which good quality metadata are provided (sampling location). In total we include 283 samples from 56 countries in the supplementary data tables.

Whilst this data set is a comprehensive overview of available $\delta^{18}O\text{-}PO_4$ data, it only covers a relatively small number of the global phosphatic lithologies detailed in the *Chernoff* and *Orris* (2002a, 2002b) mineral reserves list, which exceeds 1600 sites, if you include those derived from or related to guano deposits. This highlights a major dearth of available isotope data in comparison to the number of PO_4 reserves deemed significant enough to make the mineral reserve list. More work is needed by the community to try and develop the isotope data set. This will allow a more thorough assessment of the relationships between deposit formation mechanism, preservation history, location and isotope value and critically will enable a more reasoned assessment of potential end-member values for the soil $\delta^{18}O\text{-}PO_4$ system.

For ease of discussion, we break down the data set into the three common formation mechanisms for phosphatic lithologies rather than geographic context.

4.2 Sedimentary bedrock isotope values

The largest set of $\delta^{18}O\text{-}PO_4$ data comes from sedimentary bedrock sources with 179 samples compiled from existing literature and 32 new values from this study (Fig. 2). The data produced as part of this study include samples from 14 different countries (Tab. S1). These samples span 535 million years from the youngest, associated with the Varswater Orebody in South Africa Lower (Pliocene, 5 million years), to a sample from the Indian Lower Tal Formation (Proterozoic-Cambrian, 540 million years). The $\delta^{18}O\text{-}PO_4$ values range from +24.8‰ (Tanzania) to +10.1‰ (India). Our samples follow a distinctive trend with younger samples having higher isotope values than older ones (Fig. 2, Tab. S1). When we include sedimentary samples from the literature, this data set spans the widest geological range of all the rock types. Five extremely old samples presented in *Blake* et al. (2010) originate from the Onverwacht Group (South Africa) and are of Archean age (approx. 3.5 billion years), but the majority of the sedimentary data set spans from the Lower Proterozoic (approx. 2000 million years) to modern Holocene age sediments (Tab. S1, Fig. 2). All samples have, where possible, been classified by their geology and formation name in Tab. S1, following either the information with the original samples or based on the mineral reserves list (*Chernoff* and *Orris*, 2002a, 2002b). More modern sediments have characteristically higher isotope values (+16 to +25‰) than those more ancient deposits (+10 to +17‰) (Fig. 2). There are a few exceptions to this rule with lower isotope values being reported for modern (100–0.1 Ma) sediments. These are mostly represented in one of the oldest archives, that of *Longinelli* and *Nuti* (1968), an archive which *Pucéat* et al. (2010) suggests should be corrected when comparing to modern analytical methods. A shift of +2.2‰ would align this data set far more closely with other similar age marine sedimentary values.

Several of the older data sets, including that of *Shemesh* et al. (1988), were originally compiled to test the application of $\delta^{18}O\text{-}PO_4$ to precise ocean palaeothermometry. This dataset built on the conclusions of *Longinelli* and *Nuti* (1968) and *Shemesh* et al. (1983), who found a trend of decreasing $\delta^{18}O\text{-}PO_4$ with increasing age (Fig. 2). *Shemesh* et al. (1983) suggest that the general trend for lower $\delta^{18}O\text{-}PO_4$ values with age is driven by an equilibrium between original formation

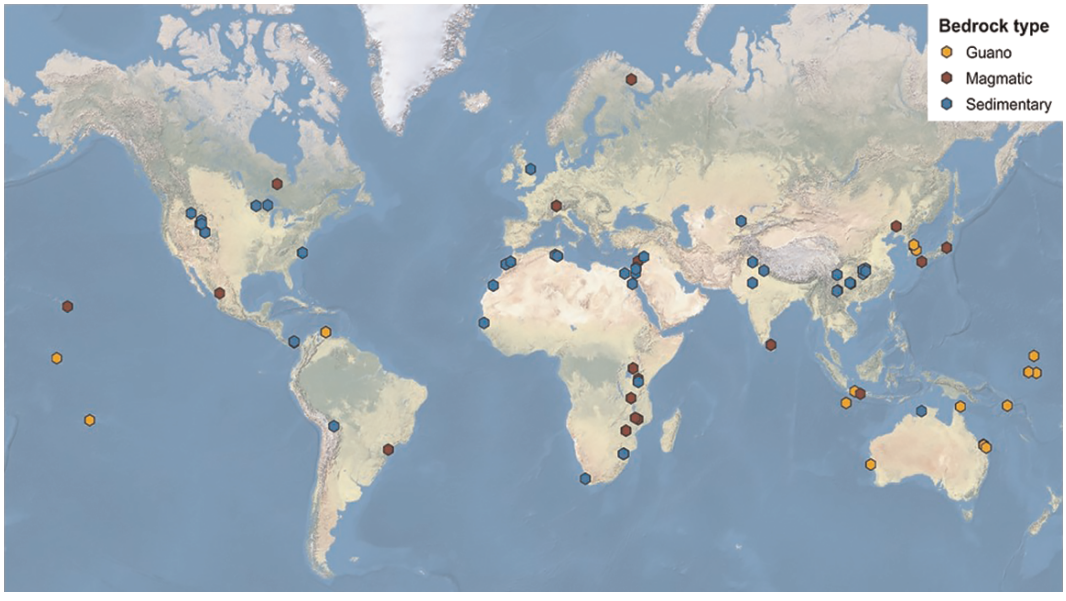

Figure 1: Global distribution of bedrocks for which geographical metadata is provided or could be obtained to a good degree of certainty. Samples where only a country name was provided are not included in this figure. Produced in QGIS 2018 (*QGIS Development Team*, 2018). For full colour please refer to the online version of the article.

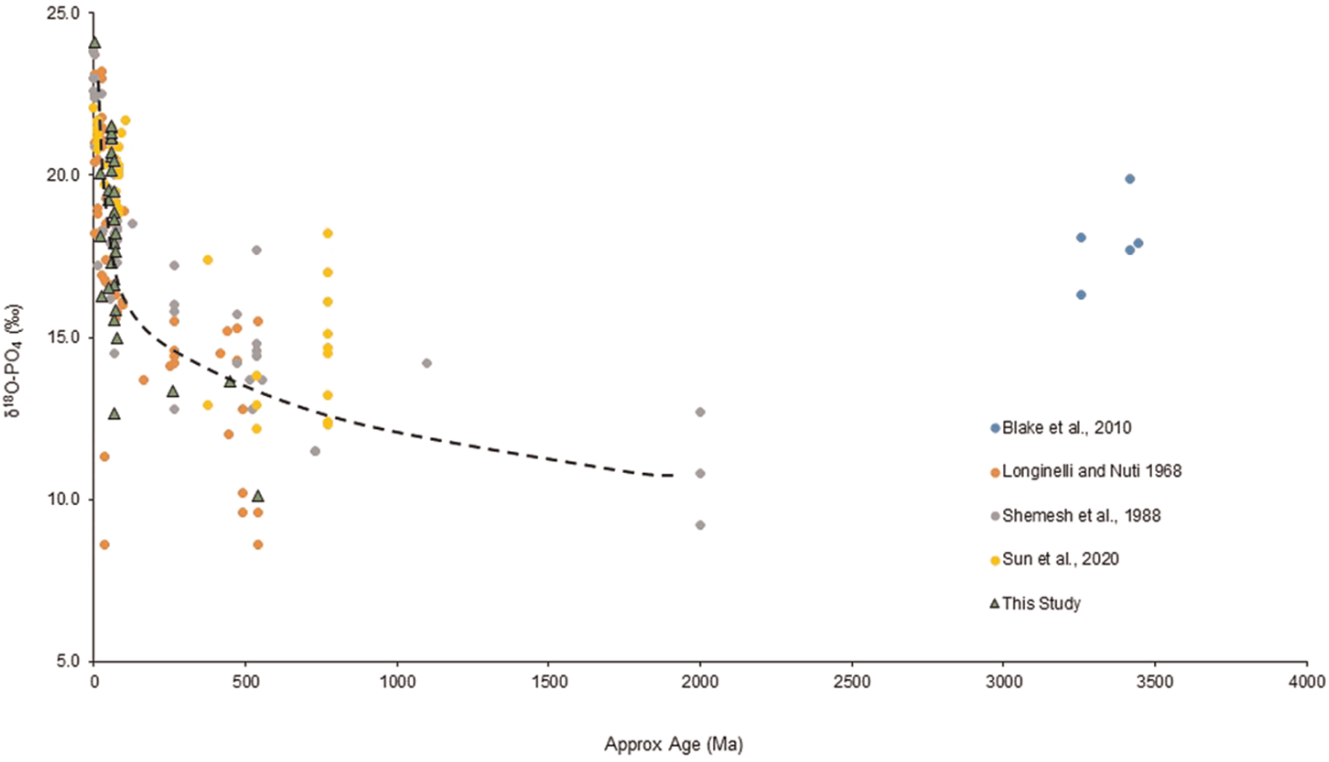

Figure 2: The δ^{18}O-PO_4 data for sedimentary sites with appropriate age information. Ages are approximate as many samples are associated with geological periods in the original literature rather than precise dates. The clear temporal trend of *Shemesh* et al. (1988) can be observed with a few lower values in the past 500 Ma, mostly associated with the study of *Longinelli* and *Nuti* (1968) and possibly related to methodologically derived offsets in the data (*Pucéat* et al., 2010). For full colour please refer to the online version of the article.

temperature and ocean water isotope value ($\delta^{18}O_{H_2O}$). They postulate that under these conditions the microbially derived Eδ^{18}O-PO_4, lying between dissolved PO_4 and $\delta^{18}O_{H_2O}$, imprinted a temperature dependent isotope signature into precipitating inorganic P minerals, much as is seen under some modern ocean conditions where P minerals form (*Colman* et al., 2005).

However, *Shemesh* et al. (1988) do caveat that some bedrocks exhibit clear isotopic disequilibrium or secondary alteration, leading to calculated formation temperatures far in excess of the natural surface conditions (> 100°C). They attribute these findings to the secondary breakdown of the bedrock mineral by biota, with microbially driven O exchange (*via* an unidentified mechanism), influencing the original δ^{18}O-PO_4 value and rendering the palaeo-thermometry technique void for some samples and locations (*Shemesh* et al., 1988). *Goldhammer* et al. (2011) show that under modern settings actively depositing marine P can be out of equilibrium with surrounding waters, this disequilibrium is not a secondary, post deposition, mechanism but controlled strongly by varying microbial uptake strategies within modern deposition settings. Studies have also shown that there is the potential for wide variations in δ^{18}O-PO_4 value over a single geological formation related to that formations geomorphology. *Hiatt* and *Budd*'s (2001) study of the Upper Permian Phosphoria Formation in the USA highlights the starkly different depositional environments of a single phosphorite formation, and whilst the δ^{18}O-PO_4 value proved useful in characterising these formation environments the authors describe a range of δ^{18}O-PO_4 values from +13.7 to +20.2‰.

The clear heterogeneity across formation and the potential for disequilibrium at the point of formation means that trying to use the sediment age to attribute a δ^{18}O-PO_4 to sedimentary bedrocks is unwise. Whilst general trends can be identified (Fig. 2), it is critically important researchers aim characterise a local bedrock endmember δ^{18}O-PO_4 value before applying the δ^{18}O-PO_4 methodology for its application as a tracer of the soil P system.

4.3 Guano deposit isotope values

Twenty eight of the deposits described here, including those from *Ayliffe* et al. (1992) and new samples (our archive) from islands in the Indian and Pacific Oceans, are classified as 'bird guano' derived (Tab. S2). This classification is descriptive of a depositional environment where there has potentially been chemical reactions between bird guano and carbonate during the development of these phosphorites, including guano derived P into the mineral phase (*Aharon* and *Veeh*, 1984). Guano deposits can roughly be split into two categories: (1) those younger (< 200,000 years) surface deposits recently formed locally from guano leaching, including phosphatic calcarenites which consist of carbonate sand and conglomerate cements with apatite, or (2) older (> 200,000 years), which consist of more or less pure apatite found in uplifted atolls with well-developed karst lithology, where

leaching of guano derived P (often following the dissolution of category one phosphate minerals) into the underlying bedrock has occurred, followed by secondary precipitation (*Ayliffe* et al., 1992; *Szilas*, 2002). Where any one deposit may lie in this categorisation is often complex to interpret and needs site specific study, and dating of these deposits is known to be complex (*Ayliffe* et al., 1992). It should be noted that, whilst we subdivide the guano data set into modern and ancient, these bird guano derived bedrocks are all relatively modern (most < 1 Ma) in comparison to sedimentary and igneous rocks.

Here we present 13 new guano derived deposits in this study (Tab. S2). All these deposits are, to the best of our knowledge, from young formations (Holocene; 11,600 –0 years BP) and have a range of δ^{18}O-PO_4 +14.7 to +19.6‰. All the other modern samples listed here are from *Ayliffe* et al. (1992) and have δ^{18}O-PO_4 values ranging between +20.1 and +22.8‰ similar to, or with slightly higher isotope values (1–2‰) than the modern bird guano collected at the same sites (+19.8 to +23.1‰) and associated with their formation (*Ayliffe* et al., 1992). *Ayliffe* et al. (1992) suggest that the slight (if not significant) difference between the modern guano and the local mineral precipitates is a result of an isotopic fractionation associated with the transformation of bird guano to apatite. This transformation is associated with microbial uptake, enzyme breakdown and cycling of P, which leaves the mineral precipitate δ^{18}O-PO_4 in near temperature dependent Eδ^{18}O-PO_4 with evaporative surface/soil waters [Eq. (1)]. More ancient island phosphorites, such as those found in emergent atolls, appear to have δ^{18}O-PO_4 values that are lower (+14.7 to +19.1‰) than the values of their assumed source guano material or local surface minerals (*Ayliffe* et al., 1992). The most convincing explanation for this lower isotope value being preserved in ancient apatite is the within karst enzymatic breakdown of guano derived P, leading to Eδ^{18}O-PO_4 with meteoric waters within the karst. These waters have a lower δ^{18}O value than that of the evaporatively enriched soils, leading to a measurable change in δ^{18}O-PO_4 in these deposits in comparison to either a bird guano or primary mineral source.

We also provide data from six cave guano deposits associated with bat colonies (Tab. S2). One of our sample set is a cave limestone (Java, Indonesia) derived from bat guano (+17.2‰), this sample is thought to be older (66 Ma) than the rest of the guano data set although dating is complex. The only comprehensive work we could find on this type of deposit is that of *Chang* et al. (2010) who describe two types of apatite deposits in South Korean caves. The first deposit type described by *Chang* et al. (2010) was an autogenic apatite formed within sediments directly below large bat guano deposits (U2-sed; Tab. S2). These apatite formations have similar δ^{18}O-PO_4 values (+21.9‰) to that of the original guano material (+21.4‰), suggesting that these deposits were not significantly metabolised by microorganisms prior to deposition, potentially due to the high concentration of P available from the large guano deposits and the direct formation of apatite from leaching guano. The second type of deposit, hydroxylapatite crusts, are isotopically much lighter (+14.6 to +15.6‰; Tab. S2) than the original guano material, attributed to the cycling of P by microorganisms and enzyme mediated O exchange, the same as the mechanism suggested by *Ayliffe* et al. (1992). Based on cave water $\delta^{18}O_{H_2O}$ and annual mean temperature, *Chang* et al. (2010) suggest that these crusts are at, or very near, expected Eδ^{18}O-PO_4, suggesting intracellular P cycling by pyrophosphatase. They hypothesise that the difference in formation mechanism between these crusts and apatites formed directly below guano deposits is due to the lower availability/limitation of P in the crusts as these are formed away from the concentrated guano deposits from bat urea. Where guano derived P is limited, this is all cycled by microbial communities, leading to the distinctive Eδ^{18}O-PO_4 end member, 6‰ lower than the original guano (*Chang* et al., 2010).

Due to the conditions of their formation the δ^{18}O-PO_4 of mineral deposits associated with both bird and bat guano samples are often influenced by microbiological cycling of P and the subsequent deposition of inorganic P. It is likely that the high prevalence of microbial biota in guano is responsible for the production of enzymes capable of facilitating the rapid breakdown of the P-O bond and the re-equilibrium with surrounding water (*Chang* et al., 2010). This abundance of microbes and the high availability of organic P in the guano clearly promotes the deposition of inorganic P rich substrates, which have undergone significant isotope exchange or complete equilibrium with surrounding waters, re-setting the original guano δ^{18}O-PO_4 signature. Therefore, those wanting to estimate an end member value for a guano derived phosphorite (which is often a local or regional source of fertiliser), understanding the age, depositional history and setting of deposition is key.

4.4 Igneous bedrock isotope values

Samples of igneous origin (39 total) have some of the most distinctive δ^{18}O-PO_4 values in the dataset, irrespective of age. These formations have a range much lower than the majority of sedimentary and guano deposits. Low δ^{18}O-PO_4 values are a result of these rocks high temperature formation mechanism, where higher temperatures have been shown to result in a negative isotope shift (*Lecuyer* et al., 1999). Samples from our archive include the lowest recorded bedrock δ^{18}O-PO_4 value reported in any of the literature, at –0.8‰. This sample was from the Tundulu complex in Malawi and is of Late Jurassic–Early Cretaceous age (Tab. S3), our archive also includes several samples from Panama, Uganda, and from Kola mine in Russia. These new data span the full range of δ^{18}O-PO_4, previously reported within the literature, –0.8 to +12.1‰ (Fig. 3, Tab. S3). However, until this study, the best single combined archive of igneous rock δ^{18}O-PO_4 values was provided in *Mizota* et al. (1992). Their study compiled the first clear archive of igneous values to act as a reference to their work focussed on understanding the relative contribution of P sources within soils of volcanic origin in Java, Indonesia and the African Rift Valley. These reference samples were collected globally and included volcanic ash, carbonatite and hydrothermal geodes (Tab. S3).

Work by *Tamburini* et al. (2012), *Angert* et al. (2012), *Helfenstein* et al. (2018), and *Shen* et al. (2020) have perhaps most successfully demonstrated the potential for δ^{18}O-PO_4 as a

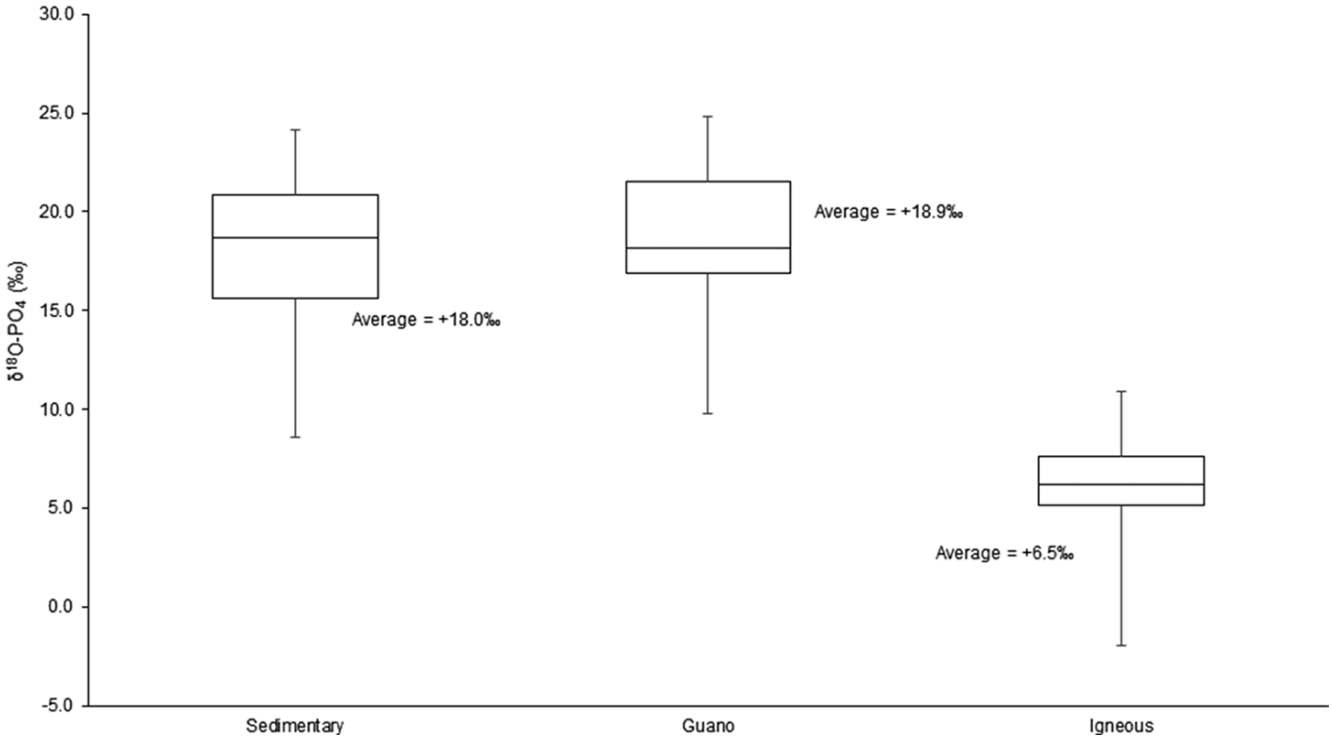

Figure 3: Box and Whisker plot of all data compiled within the study showing maximum, median, upper and lower quartile and minimum isotope values for each bedrock type. This clearly demonstrates the isotopic difference between igneous and bedrocks of other formation mechanism.

tracer of enhanced microbial cycling of P and the re-setting of the source δ^{18}O-PO_4 signature with an igneous bedrock endmember. Each of these studies have focussed on assessing P cycling over a rainfall gradient or during initial colonisation of a region. Most characteristically, each has an igneous bedrock endmember, isotopically quite distinctive from the values expected to be encountered if Eδ^{18}O-PO_4 existed due to enzymatic breakdown by pyrophosphatase [Eq. (1)]. As igneous bedrock values are much lower than those of guano and sedimentary deposits (Fig. 3), this divergence is more prominent and P cycling more apparent when it occurs. *Shen* et al. (2020) highlight that fractionations associated with DNA and RNA hydrolysis (–25 and –5‰, respectively), alkaline and acid phosphatases (approx. –25‰), and 5'-nucleotidase hydrolysis (–10‰) all cause a negative shift in isotope values (*Liang* and *Blake*, 2006), whilst inorganic pyrophosphatase will cause a positive shift based on equilibrium at most modern temperature and $\delta^{18}O_{H_2O}$ combinations. Therefore, highly positive isotope values (+20 to +25‰), which have been significantly shifted away from an igneous bedrock endmember can only reasonably be attributed to the microbial cycling of P *via* inorganic pyrophosphatase (*Shen* et al., 2020).

4.5 Inter study comparison

This combined data set facilitates the opportunity to assess the homogeneity of published isotope data at geological structures, where several samples have been independently collected and analysed. For some locations we have samples from the same geological structure but that have been collected, stored and prepared at different times and in different places, as well as being analysed by different researchers, following different methodologies (Tabs. S1–3). Comparisons across these data sets give a far more robust idea of the expected heterogeneity across geological structures and methods. Based on the 10 sites where cross study comparison was possible (Tab. 1), an average 1stdv of ± 1.25‰ appears to be representative with a maximum recorded error at any one site of ± 3.78‰ (Minjingu, n = 4). We therefore suggest that workers who wish to attribute an end member value based on this data set or secondary literature, consider this level of error as a reasonable starting point, where direct analysis of δ^{18}O-PO_4 endmembers is not possible.

These data consider all possible forms of error, from heterogeneity across the geological structure, sampling inconstancies, purification and analytical error. It should be highlighted that much of this error could be associated with heterogeneity within the geological structure as demonstrated by (*Hiatt* and *Budd*, 2001) at the Phosphoria formation, USA. The wide range of isotope values presented in their study relate to differing depositional environments across this large geological deposit and are therefore to be expected. The other site with significant differences in δ^{18}O-PO_4 is the Minjingu guano deposit in Tanzania. These samples were included in Tab. 1 to highlight the potential for isotopic heterogeneity in guano derived formations, possibly due both to variable formation conditions over 1000's of years and the unquantified extent of isotope exchange during leaching. Most of the formations, however, are either less geologically massive than the Phosphoria or less complex in formation history than Minjingu. Where these have been sampled over multiple studies, we generally observe a reduced heterogeneity (Tab. 1).

Table 1: Sites where 2 or more samples have been obtained from the same geological structure, either within one or more than one study. *The Phosphoria Formation samples of *Hiatt* and *Budd* (2001) have been averaged by the 4 locations where multiple depths for each location were provided in the original text.

Formation name	Location	Geology	Average $\delta^{18}O\text{-}PO_4$ (‰)	1 stdv (‰)	Studies
Phosphoria Formation*	Idaho / Utah / Wyoming	Sedimentary	15.67 (n = 9)	1.82	*Shemesh* et al. (1988); *Hiatt* and *Budd* (2001); this study
Gafsa	Tunisia	Sedimentary	20.58 (n = 7)	1.52	this study
Puglia	Italy	Sedimentary	20.37 (n = 6)	1.36	*Longinelli* and *Nuti* (1968)
Nauru	Nauru Island	Guano	16.87 (n = 6)	1.15	*Ayliffe* et al. (1992); this study
Kola	Russia	Igneous	4.76 (n = 6)	1.36	*Sun* et al. (2020); this study
Minjingu	Tanzania	Guano	20.36 (n = 4)	3.78	this study
Arad	Israel	Sedimentary	19.57 (n = 3)	0.84	*Shemesh* et al. (1988); *Sun* et al. (2020)
Taiba	Senegal	Sedimentary	19.77 (n = 3)	0.75	*Sun* et al. (2020); this study
Oron	Israel	Sedimentary	20.55 (n = 2)	0.49	*Shemesh* et al. (1988); *Sun* et al. (2020)
Dorowa	Zimbabwe	Igneous	5.15 (n = 2)	0.21	*Mizota* et al. (1992); this study
Eppawala	Sri Lanka	Igneous	12.14 (n = 2)	0.09	*Mizota* et al. (1992); this study
Capinota	Bolivia	Sedimentary	14.66 (n = 2)	1.47	*Shemesh* et al. (1988); this study

Considering that many of these studies follow divergent sampling, purification and analysis protocols, such a level of homogeneity is promising and suggests that unless a site has distinct heterogeneity associated with the original depositional environment that using the isotope value of existing literature with appropriate error consideration can accurately reflect the $\delta^{18}O\text{-}PO_4$ of that structure. This gives significant confidence to studies using previously published isotope data to constrain endmembers to their $\delta^{18}O\text{-}PO_4$ system.

5 Conclusion

Based on a number of new bedrock $\delta^{18}O\text{-}PO_4$ isotope analyses and a comprehensive compilation of existing literature we identify the following trends in bedrock $\delta^{18}O\text{-}PO_4$ signature both over time and between formation mechanisms.

- Igneous bedrocks have lower $\delta^{18}O\text{-}PO_4$ values than either sedimentary or guano, and these are often distinct from the $E\delta^{18}O\text{-}PO_4$ expected from the breakdown of P-O by the intracellular enzyme pyrophosphatase.
- Sedimentary and guano deposit $\delta^{18}O\text{-}PO_4$ is strongly influenced by microbial uptake and enzymatic breakdown of P both during formation and as a secondary effect after deposition, resulting in a $\delta^{18}O\text{-}PO_4$ value toward $E\delta^{18}O\text{-}PO_4$.

This information will prove invaluable to those wishing to understand bedrock $\delta^{18}O\text{-}PO_4$ as an endmember to their soil P system. Whilst this is now the most comprehensive archive of geological $\delta^{18}O\text{-}PO_4$ data and we have been able to compile data from 285 samples representing many globally important reserves, this is still a sparse dataset in comparison with the number of major P deposits found worldwide (*Chernoff* and *Orris*, 2002a, 2002b). Importantly, the range of geological bedrock $\delta^{18}O\text{-}PO_4$ values is diverse (+24.8 to –0.8‰) meaning that studies may decide to focus their research in areas which will provide a bedrock $\delta^{18}O\text{-}PO_4$ starting point for maximum potential change due to P cycling. When aiming to characterise the bedrock $\delta^{18}O\text{-}PO_4$ for soil P cycling investigations we strongly suggest the following working procedure: (1) undertake a primary characterisation of endmember $\delta^{18}O\text{-}PO_4$ at the study site; (2) where this is not possible, but data from the same geological formation has been published, use this, incorporating a working error of $\pm$ 1.25‰ associated with within formation heterogeneity; (3) if no data are available for the specific geological formation of interest, consider its formation mechanism and age, this should provide a robust starting point for $\delta^{18}O\text{-}PO_4$ estimation. Following this procedure should enable the most accurate method for endmember estimation. Whilst this data set is a good start, much further work is still required by the community to characterise the $\delta^{18}O\text{-}PO_4$ values of major global P reserves and the effect of converting mineral P to fertilisers through chemical treatment, which may impart a hitherto unknown isotopic effect on the source P mineral.

Acknowledgments

This work was supported by the *2015 Rothamsted Fellowship*. We thank *Don Appleton* at the British Geological Survey (BGS) and *John McArthur* (University College London) for access to samples from their own collections and the Lawes Agricultural Trust and Rothamsted Research for access to samples from the Rothamsted Long-term Sample Archive.

The Rothamsted Long-term Sample Archive is supported by the *UKRI* (*UK Research and Innovation*), *BBSRC* (*Biotechnology and Biological Sciences Research Council*, *BBS/E/C/000I0330*), and the *Lawes Agricultural Trust*. The stable isotope analysis was funded as part of *NEIF grant IP-1807-0618*.

Data Availability Statement

The data that supports the findings of this study are available in the supplementary material of this article.

References

Aharon, P., *Veeh, H. H.* (1984): Isotope studies of insular phosphates explain atoll phosphatization. *Nature* 309, 614–617.

Angert, A., *Weiner, T.*, *Mazeh, S.*, *Sternberg, M.* (2012): Soil phosphate stable oxygen isotopes across rainfall and bedrock gradients. *Environ. Sci. Technol.* 46, 2156–2162.

Ayliffe, L. K., *Veeh, H. H.*, *Chivas, A. R.* (1992): Oxygen isotopes of phosphate and the origin of island apatite deposits. *Earth Planet. Sci. Lett.* 108, 119–129.

Bauke, S. L. (2021): Oxygen isotopes in phosphate—The key to phosphorus tracing? *J. Plant Nutr. Soil Sci.* 184, 12–19.

Blake, R. E., *Chang, S. J.*, *Lepland, A.* (2010): Phosphate oxygen isotopic evidence for a temperate and biologically active Archaean ocean. *Nature* 464, 1029–1032.

Blake, R. E., *O'Neil, J. R.*, *Surkov, A. V.* (2005): Biogeochemical cycling of phosphorus: Insights from oxygen isotope effects of phosphoenzymes. *Am. J. Sci.* 305, 596–620.

Chang, S. J., *Blake, R. E.* (2015): Precise calibration of equilibrium oxygen isotope fractionations between dissolved phosphate and water from 3 to 37°C. *Geochim. Cosmochim. Ac.* 150, 314–329.

Chang, S. J., *Blake, R. E.*, *Stout, L. M.*, *Kim, S. J.* (2010): Oxygen isotope, micro-textural and molecular evidence for the role of microorganisms in formation of hydroxylapatite in limestone caves, South Korea. *Chem. Geol.* 276, 209–224.

Chernoff, C. B., *Orris, G. J.* (2002a): Data Set of World Phosphate Mines, Deposits, and Occurrences: Part A. Geologic Data. US Department of the Interior, US Geological Survey, Washington, DC, USA.

Chernoff, C. B., *Orris, G. J.* (2002b): Data Set of World Phosphate Mines, Deposits, and Occurrences: Part B. Location and Mineral Economic Data. US Department of the Interior, US Geological Survey, Washington, DC, USA.

Cohn, M. (1957): Phosphate–water exchange reaction catalyzed by inorganic pyrophosphatase of yeast. *J. Biol. Chem.* 230, 369–379.

Colman, A. S., *Blake, R. E.*, *Karl, D. M.*, *Fogel, M. L.*, *Turekian, K. K.* (2005): Marine phosphate oxygen isotopes and organic matter remineralization in the oceans. *Proc. Natl. Acad. Sci. USA* 102, 13023–13028.

Davies, C. L., *Surridge, B. W. J.*, *Gooddy, D. C.* (2014): Phosphate oxygen isotopes within aquatic ecosystems: Global data synthesis and future research priorities. *Sci. Total Environ.* 496, 563–575.

George, T. S., *Giles, C. D.*, *Menezes-Blackburn, D.*, *Condron, L. M.*, *Gama-Rodrigues, A. C.*, *Jaisi, D.*, *Lang, F.*, *Neal, A. L.*, *Stutter, M. I.*, *Almeida, D. S.*, *Bol, R.*, *Cabugao, K. G.*, *Celi, L.*, *Cotner, J. B.*, *Feng, G.*, *Goll, D. S.*, *Hallama, M.*, *Krueger, J.*, *Plassard, C.*, *Rosling, A.*, *Darch, T.*, *Fraser, T.*, *Giesler, R.*, *Richardson, A. E.*, *Tamburini, F.*, *Shand, C. A.*, *Lumsdon, D. G.*, *Zhang, H.*, *Blackwell, M. S. A.*, *Wearing, C.*, *Mezeli, M. M.*, *Almås, Å. R.*, *Audette, Y.*, *Bertrand, I.*, *Beyhaut, E.*, *Boitt, G.*, *Bradshaw, N.*, *Brearley, C. A.*, *Bruulsema, T. W.*, *Ciais, P.*, *Cozzolino, V.*, *Duran, P. C.*, *Mora, M. L.*, *de Menezes, A. B.*, *Dodd, R. J.*, *Dunfield, K.*, *Engl, C.*, *Frazão, J. J.*, *Garland, G.*, *González Jiménez, J. L.*, *Graca, J.*, *Granger, S. J.*, *Harrison, A. F.*, *Heuck, C.*, *Hou, E. Q.*, *Johnes, P. J.*, *Kaiser, K.*, *Kjær, H. A.*, *Klumpp, E.*, *Lamb, A. L.*, *Macintosh, K. A.*, *Mackay, E. B.*, *McGrath, J.*, *McIntyre, C.*, *McLaren, T.*, *Mészáros, E.*, *Missong, A.*, *Mooshammer, M.*, *Negrón, C. P.*, *Nelson, L. A.*, *Pfahler, V.*, *Poblete-Grant, P.*, *Randall, M.*, *Seguel, A.*, *Seth, K.*, *Smith, A. C.*, *Smits, M. M.*, *Sobarzo, J. A.*, *Spohn, M.*, *Tawaraya, K.*, *Tibbett, M.*, *Voroney, P.*, *Wallander, H.*, *Wang, L.*, *Wasaki, J.*, *Haygarth, P. M.* (2017): Organic phosphorus in the terrestrial environment: a perspective on the state of the art and future priorities. *Plant Soil* 427, 191–208.

Goldhammer, T., *Brunner, B.*, *Bernasconi, S. M.*, *Ferdelman, T. G.*, *Zabel, M.* (2011): Phosphate oxygen isotopes: Insights into sedimentary phosphorus cycling from the Benguela upwelling system. *Geochim. Cosmochim. Ac.* 75, 3741–3756.

Gooddy, D. C., *Lapworth, D. J.*, *Bennett, S. A.*, *Heaton, T. H. E.*, *Williams, P. J.*, *Surridge, B. W. J.* (2016): A multi-stable isotope framework to understand eutrophication in aquatic ecosystems. *Water Res.* 88, 623–633.

Granger, S. J., *Heaton, T. H. E.*, *Pfahler, V.*, *Blackwell, M. S. A.*, *Yuan, H.*, *Collins, A. L.* (2017): The oxygen isotopic composition of phosphate in river water and its potential sources in the Upper River Taw catchment, UK. *Sci. Total Environ.* 574, 680–690.

Granger, S. J., *Yang, Y.*, *Pfahler, V.*, *Hodgson, C.*, *Smith, A. C.*, *Le Cocq, K.*, *Collins, A. L.*, *Blackwell, M. S. A.*, *Howden, N. J. K.* (2018): The stable oxygen isotope ratio of resin extractable phosphate derived from fresh cattle faeces. *Rapid Commun. Mass Spectrom.* 32, 703–710.

Helfenstein, J., *Tamburini, F.*, *Von Sperber, C.*, *Massey, M. S.*, *Pistocchi, C.*, *Chadwick, O. A.*, *Vitousek, P. M.*, *Kretzschmar, R.*, *Frossard, E.* (2018): Combining spectroscopic and isotopic techniques gives a dynamic view of phosphorus cycling in soil. *Nat. Commun.* 9. DOI: https://doi.org/10.1038/s41467-018-05731-2.

Hiatt, E. E., *Budd, D. A.* (2001): Sedimentary phospate formation in warm shallow waters: New insights into the palaeoceanography of the Permian Phosphoria Sea from analysis of phosphate oxygen isotopes. *Sediment. Geol.* 145, 119–133.

Jaisi, D. P. (2013): Stable isotope fractionations during reactive transport of phosphate in packed-bed sediment columns. *J. Contam. Hydrol.* 154, 10–19.

Jaisi, D. P., *Blake, R. E.* (2010): Tracing sources and cycling of phosphorus in Peru Margin sediments using oxygen isotopes in authigenic and detrital phosphates. *Geochim. Cosmochim. Ac.* 74, 3199–3212.

Jaisi, D. P., *Blake, R. E.*, *Kukkadapu, R. K.* (2010): Fractionation of oxygen isotopes in phosphate during its interactions with iron oxides. *Geochim. Cosmochim. Ac.* 74, 1309–1319.

Lecuyer, C., *Grandjean, P.*, *Sheppard, S. M. F.* (1999): Oxygen isotope exchange between dissolved phosphate and water at temperatures ≤ 135°C: inorganic *versus* biological fractionations. *Geochim. Cosmochim. Ac.* 63, 855–862.

Li, H., *Jaisi, D. P.* (2015): An isotope labeling technique to investigate atom exchange during phosphate sorption and desorption. *Soil Sci. Soc. Am. J.* 79, 1340–1351.

Liang, Y., *Blake, R. E.* (2006): Oxygen isotope composition of phosphate in organic compounds: Isotope effects of extraction methods. *Org. Geochem.* 37, 1263–1277.

Liang, Y., *Blake, R. E.* (2009): Compound- and enzyme-specific phosphodiester hydrolysis mechanisms revealed by $\delta^{18}O$ of dissolved

inorganic phosphate: Implications for marine P cycling. *Geochim. Cosmochim. Ac.* 73, 3782–3794.

Longinelli, A., *Nuti, S.* (1968): Oxygen isotopic composition of phosphorites from marine formations. *Earth Planet. Sci. Lett.* 5, 13–16.

McLaughlin, K., *Cade-menun, B. J.*, *Paytan, A.* (2006): The oxygen isotopic composition of phosphate in Elkhorn Slough, California: A tracer for phosphate sources. *Estuar. Coast. Shelf Sci.* 70, 499–506.

McLaughlin, K., *Paytan, A.*, *Kendall, C.*, *Silva, S.* (2006): Oxygen isotopes of phosphatic compounds—Application for marine particulate matter, sediments and soils. *Mar. Chem.* 98, 148–155.

Mizota, C., *Domon, Y.*, *Yoshida, N.* (1992): Oxygen isotope composition of natural phosphates from volcanic ash soils of the Great Rift Valley of Africa and east Java, Indonesia. *Geoderma* 53, 111–123.

O'Neil, J. R., *Vennemann, T. W.*, *McKenzie, W. F.* (2003): Effects of speciation on equilibrium fractionations and rates of oxygen isotope exchange between $(PO_4)_{aq}$ and H_2O. *Geochim. Cosmochim. Ac.* 67, 3135–3144.

Pistocchi, C., *Mészáros, É.*, *Tamburini, F.*, *Frossard, E.*, *Bünemann, E. K.* (2018): Biological processes dominate phosphorus dynamics under low phosphorus availability in organic horizons of temperate forest soils. *Soil Biol. Biochem.* 126, 64–75.

Pistocchi, C., *Tamburini, F.*, *Gruau, G.*, *Ferhi, A.*, *Trevisan, D.*, *Dorioz, J. M.* (2017): Tracing the sources and cycling of phosphorus in river sediments using oxygen isotopes: Methodological adaptations and first results from a case study in France. *Water Res.* 111, 346–356.

Pucéat, E., *Joachimski, M. M.*, *Bouilloux, A.*, *Monna, F.*, *Bonin, A.*, *Motreuil, S.*, *Morinière, P.*, *Hénard, S.*, *Mourin, J.*, *Dera, G.* (2010): Revised phosphate–water fractionation equation reassessing paleotemperatures derived from biogenic apatite. *Earth Planet. Sci. Lett.* 298, 135–142.

Pufahl, P., *Groat, L.* (2017): Sedimentary and igneous phosphate deposits: formation and exploration: an invited paper. *Econ. Geol.* 112, 483–516.

QGIS Development Team (2018): QGIS Geographic Information System. Open Source Geospatial Foundation Project. Available at: https://qgis.org/en/site/

Ruttenberg, K. C. (2003): The Global Phosphorus Cycle, in Holland, H. D., Turekian, K. K. (eds.): Treatise on Geochemistry. Elsevier, Amsterdam, The Netherlands, pp. 585–633.

Shemesh, A., *Kolodny, Y.*, *Luz, B.* (1983): Oxygen isotope variations in phosphate of biogenic apatites, II. Phosphorite rocks. *Earth Planet. Sci. Lett.* 64, 405–416.

Shemesh, A., *Kolodny, Y.*, *Luz, B.* (1988): Isotope geochemistry of oxygen and carbon in phosphate and carbonate of phosphorite francolite. *Geochim. Cosmochim. Ac.* 52, 2565–2572.

Shen, J., *Smith, A. C.*, *Claire, M. W.*, *Zerkle, A. L.* (2020): Unravelling biogeochemical phosphorus dynamics in hyperarid Mars analogue soils using stable oxygen isotopes in phosphate. *Geobiology* 18, 760–779.

Szilas, C. (2002): The Tanzanian Minjingu Phosphate Rock. Royal Veterinary and Agricultural University Copenhagen, Copenhagen, Denmark.

Tamburini, F., *Bernasconi, S. M.*, *Angert, A.*, *Weiner, T.*, *Frossard, E.* (2010): A method for the analysis of the δ18O of inorganic phosphate extracted from soils with HCl. *Eur. J. Soil Sci.* 61, 1025–1032.

Tamburini, F., *Pfahler, V.*, *Bünemann, E. K.*, *Guelland, K.*, *Bernasconi, S. M.*, *Frossard, E.* (2012): Oxygen isotopes unravel the role of microorganisms in phosphate cycling in soils. *Environ. Sci. Technol.* 46, 5956–5962.

Tamburini, F., *Pfahler, V.*, *von Sperber, C.*, *Frossard, E.*, *Bernasconi, S. M.* (2014): Oxygen isotopes for unraveling phosphorus transformations in the soil–plant system: A review. *Soil Sci. Soc. Am. J.* 78, 38–46.

Van Kauwenbergh, S. J. (2010): World Phosphate Rock Reserves and Resources. Technical Bulletin IFDC-T-75. IFCD, Muscle Shoals, AL, USA.

Vennemann, T. W., *Fricke, H. C.*, *Blake, R. E.*, *O'Neil, J. R.*, *Colman, A.* (2002): Oxygen isotope analysis of phosphates: A comparison of techniques for analysis of Ag_3PO_4. *Chem. Geol.* 185, 321–336.

Von Sperber, C., *Kries, H.*, *Tamburini, F.*, *Bernasconi, S. M.*, *Frossard, E.* (2014): The effect of phosphomonoesterases on the oxygen isotope composition of phosphate. *Geochim. Cosmochim. Ac.* 125, 519–527.

Walker, T. W., *Syers, J. K.* (1976): The fate of phosphorus during pedogenesis. *Geoderma* 15, 1–19.

